Photochemical energy conversion: from molecular dyads to solar cells

James R. Durrant,*[a] Saif A. Haque[a] and Emilio Palomares[ab]

Received (in Cambridge, UK) 6th February 2006, Accepted 7th April 2006
First published as an Advance Article on the web 8th May 2006
DOI: 10.1039/b601785c

Photochemical approaches to solar energy conversion are currently making rapid progress, increasing not only academic but also commercial interest in molecular-based photovoltaic solar cells. This progress has been achieved not only by increased understanding of the physics and physical chemistry of device function but also through advances in chemical and materials synthesis and processing, which now allows the design and fabrication of increasingly sophisticated device structures organised on the nanometer length scale. In this feature article, we review some progress in this field, focusing in particular upon the electron-transfer dynamics which underlie the function of dye-sensitised, nanocrystalline solar cells. The article starts by building upon the parallels between the function of such devices and the function of simple donor/acceptor molecular systems in solution. We then go on to discuss the optimisation of device function, and in particular the use of self-assembly-based strategies to control interfacial electron-transfer kinetics.

1 Introduction

The reaction centres of photosynthetic organisms are undoubtedly the most sophisticated examples of photochemical energy conversion systems. They have inspired chemists to synthesise artificial photosynthetic systems capable of emulating at least key elements of their function. Perhaps the simplest example of such photosynthetic models systems are molecular donor/acceptor complexes. In such complexes, optical excitation initiates an electron-transfer reaction from a molecular donor, D, to a molecular acceptor, A, resulting in a charge separated radical pair state D^+A^-. Extensive studies of such donor/acceptor systems in solution have led to a detailed understanding of their structure/function relationship in terms of non-adiabatic electron-transfer theory.[1] This has in turn led to impressive advances in the molecular control of electron-transfer dynamics in such systems,[2] such as the recent reports of remarkably efficient, long-lived charge separation for simple molecular donor/acceptor dyads by Fukuzumi *et al.*,[3] as illustrated in Fig. 1.

In parallel with these studies of molecular donor/acceptor systems, attention has increasingly turned to the possibility of fabricating photovoltaic solar cells based upon molecular or

[a]*Department of Chemistry, Imperial College London, Exhibition Road, London, UK SW7 2AZ. E-mail: j.durrant@imperial.ac.uk; Fax: 44 20 7594 5801*
[b]*Institut Català d'Investigació Química. Avda. Països Catalans, 16. Tarragona. C.P. 43007, Tarragona, Spain*

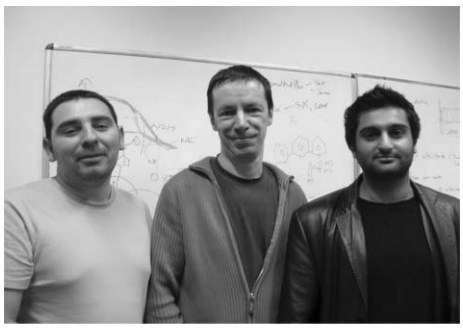

Emilio J. Palomares, James Durrant and Saif Haque

James Durrant is Professor of Photochemistry in the Department of Chemistry at Imperial College London. After completing his undergraduate studies in Physics from the University of Cambridge, he obtained a PhD in Biochemistry at Imperial College London in 1991, studying the primary reactions of plant photosynthesis. After postdoctoral positions and a BBSRC Advanced Fellowship, he joined the Chemistry Department at Imperial College in 1999. His interests are photochemical approaches to solar energy conversion, electron-transfer dynamics and excitonic solar cells.

Saif Haque is a Royal Society University Research Fellow in the Department of Chemistry at Imperial College London. After undergraduate studies in Chemistry, he completed his PhD at Imperial College in 2000, studying charge recombination in dye-sensitised solar cells. After five years of post-doctoral research, he was awarded his Fellowship in 2005. His research interests involve the photophysical characterization and application of nanostructured molecular materials.

Emilio J. Palomares received his PhD in Chemistry from the University Politècnica de Valencia in 2001. He worked as Marie Curie Postdoctoral Fellow at the Centre for Electronic Materials and Devices at Imperial College in London. In 2004 he returned to Spain as Ramon y Cajal Fellow at the Insitituto de Ciencia Molecular, Universidad de Valencia (ICMol-UV) and in 2006 he moved as a Project Leader to the Institut Català d'Invesitgació Química (ICIQ) where he is working on light-induced molecular and bio-molecular devices.

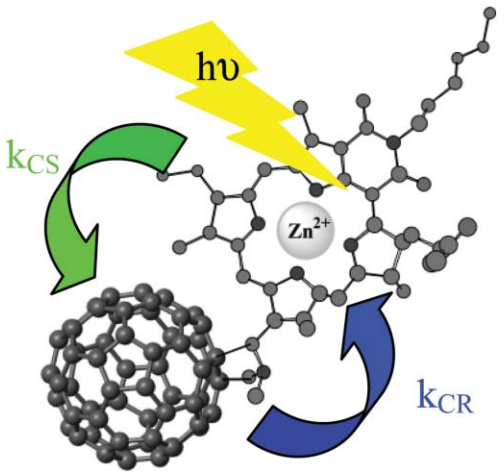

Fig. 1 Illustration of charge separation and recombination in a zinc chlorine/fullerene molecular dyad. Optical excitation of the chlorine results in electron transfer to the fullerene with a rate constant $k_{CS} \sim 10^{11}\ s^{-1}$. The free energy of the resulting charge separated state is ~1.3 eV (70% of the energy of the chlorine singlet excited state). This charge separated state exhibits a lifetime of 200 μs at room temperature ($k_{CR} = 5 \times 10^3\ s^{-1}$). Adapted from ref. 1*c*.

polymer light absorbers.[4] Such studies are being given added impetus by concerns over the environmental impact of our dependence upon fossil fuels, and by concerns that the high capital cost and long energy payback times of photovoltaic cells based upon crystalline silicon may limit the practicality of such devices for large-scale renewable energy production. Molecular-based solar cells offer the potential for efficient solar energy conversion using low-cost materials and fabrication techniques. Significant progress is now being made towards the commercial production of such devices for specific market applications.[4] However at present the efficiencies and durabilities of molecular and polymer-based devices remain modest in comparison to silicon-based solar cells, and much research and development work remains to be undertaken before such devices can effectively compete with silicon devices for large scale solar energy conversion.

In molecular (and polymer) based solar cells, the excited state generated by light absorption is a molecular, and therefore bound, excited state or 'exciton' (for this reason such devices are often referred to as 'excitonic' solar cells). This contrasts to crystalline silicon-based devices, where light absorption leads directly to the generation of free conduction band electrons and valence band holes. Charge separation of the exciton in molecular-based solar cells therefore requires electron transfer between electron donor and acceptor species within the photoactive layer of the device. As such, the underlying function of molecular solar cells has close parallels to electron-transfer dynamics of simple molecular donor/acceptor systems in solution.

In photosynthetic systems, the free energy stored in the charge separated state D^+A^- is employed to generate energy-rich chemical products. In plant photosynthesis, for example, the reducing potential stored in the reduced electron acceptor is ultimately utilised in the reduction of carbon dioxide to sugars, whilst the oxidising potential of the oxidised donor is utilised to oxidise water to molecular oxygen. In contrast, in photovoltaic systems, the donor/acceptor interface must be coupled to an external electrical circuit. This requires the transport of charge separated electrons and 'holes' (*i.e.*: the positive charge on the donor) to device electrodes. In such photovoltaic devices, the free energy stored in the charge separated state determines the maximum photovoltage which can be generated by the device, whilst the quantum efficiency of charge separation and transport determines the device photocurrent. Charge recombination losses (such as k_{CR} in Fig. 1) reduce the efficiency of charge collection, and therefore often limit device efficiency.

The successful 'wiring' of molecular scale donor/acceptor interfaces to macroscopic external circuits is key to the development of efficient molecular-based photovoltaic devices. Several different concepts are currently being explored to achieve this 'wiring'. The most established example of such devices is that of dye-sensitised solar cells[5] (DSSC), based on the self-assembly of a monolayer of molecular light absorbers on high surface area electrodes based on nanocrystalline, mesoporous metal oxides, as illustrated in Fig. 2. Optical excitation of the dye leads to electron injection into the conduction band of the metal oxide. Subsequently electrons are transported to the external circuit through the metal oxide film, whilst a hole transporting material or redox electrolyte inserted into the film pores serves to re-reduce the photo-oxidised dye and transport the resulting positive charge to the counter-electrode. Efficiencies of up to 11% have been reported for DSSC employing liquid electrolytes,[5] although efficiencies for solid-state (or 'quasi-solid state') devices (more attractive for most technological applications) remain more modest, in the 3–8% range depending upon materials employed.[6] An alternative device configuration (the 'bulk heterojunction' concept) is based upon a photoactive layer comprising a partially phase segregated blend of a light absorbing, hole transporting polymer with an electron transport material, typically a fullerene (C_{60}) derivative.[7] Blending

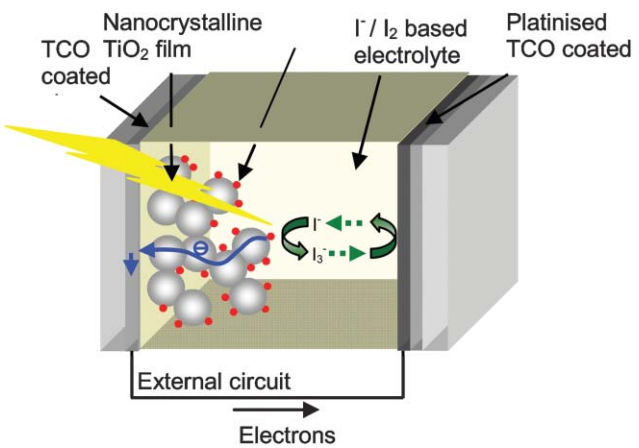

Fig. 2 Schematic of dye-sensitised solar cells. The TiO_2 nanocrystals typically have a diameter of ~15 nm, giving a surface area enhancement of up to 1000 for a 10 μm thick film. The I^-/I_2 redox electrolyte may comprise a liquid or more solid-state alternatives such as gelled ionic liquids and polymer electrolytes, or be replaced by a molecular hole conductor.

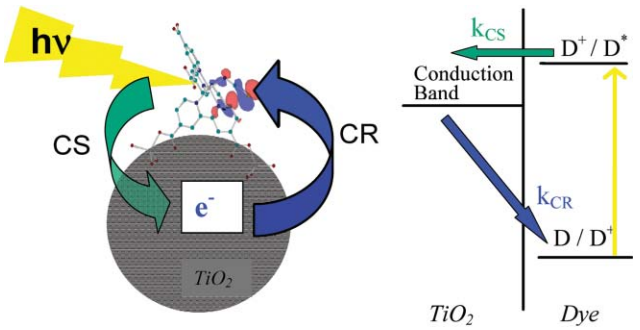

Fig. 3 Illustration of the structure, energetics and kinetics for the sensitiser dye $Ru(dcbpy)_2(NCS)_2$ adsorbed to nanocrystalline TiO_2 films.

of the donor (polymer) and acceptor (fullerene) species on the nanometer scale is essential to achieve efficient exciton dissociation. Efficiencies of >4% have been reported for such bulk heterojunction devices.[8] Finally, and most simply, devices have been fabricated from molecular donor/acceptor bilayers, employing materials chosen to achieve efficient exciton transfer to the interface without the need for blending (nanostructuring) the donor/acceptor interface.[9] All of these device concepts are now receiving extensive academic and commercial interest, and the reader is referred to elsewhere for detailed reviews of their function and technological development.[4]

This article is written from a chemist's viewpoint, with the hope of informing and motivating, in particular, the synthetic and materials chemists who are central to the further development of molecular photovoltaics. With this in mind, we address the parallels between the photochemical properties of simple molecular donor/acceptor systems and the function of molecular-based photovoltaic devices, focusing upon our recent studies of the function and optimisation of dye-sensitised, nanocrystalline solar cells.

2 A donor/acceptor model system for molecular photovoltaics

The paradigm sensitizer molecule for solution-based photochemistry is ruthenium tris-bipyridine. This organometallic dye combines strong visible light absorption and excellent photochemical stability with high photochemical reactivity, typically initiated by electron or resonance energy transfer from the triplet excited state of the dye. Ruthenium bipyridyl photochemistry has found a natural extension to molecular photovoltaics as the sensitiser dye in dye-sensitised solar cells. The first efficient ($\gg$1%) dye-sensitised photovoltaic devices were all based upon ruthenium bipyridyl sensitisation of nanocrystalline TiO_2 films and despite extensive studies of alternative sensitiser dyes and metal oxide films, devices based upon this materials combination remain the most efficient molecular photovoltaic devices reported to date.[10] Ruthenium bipyridyl sensitised nanocrystalline TiO_2 films therefore form a natural starting point for our discussion of the parallels between solution-based donor/acceptor systems and complete photovoltaic devices.

Fig. 3 illustrates the structure and photochemical function of this simple model system, where the sensitiser dye is the $Ru(bpy)_3$ analogue $RuL_2(NCS)_2$ where L is 4,4′-dicarboxy-2,2′-bipyridyl. The carboxylate groups of the dye ensure strong dye binding to the surface of the TiO_2, conformally coating the mesoporous film with a single dye monolayer. The inclusion of two NCS groups in the dye results in a significant red shift of the dye absorption, increasing the spectral overlap with solar irradiation.

Optical excitation of $RuL_2(NCS)_2$ coated TiO_2 films results in rapid electron injection from the dye excited state into the conduction band of the metal oxide, generating the charge-separated state $dye^+/e^-_{TiO_2}$.[10,11] Typical data for the dynamics of this charge separation and decay dynamics of the charge separated state due to interfacial charge recombination are shown in Fig. 4. It is apparent from these data that the electron-transfer dynamics across the dye/TiO_2 interface are temporally highly asymmetric, with the dynamics of charge separation being $\sim 10^9$-fold faster than the corresponding charge recombination reaction (*i.e.*: the interface is highly rectifying). This high asymmetry is undoubtedly a key factor enabling the high energy conversion efficiencies achieved by solar cells based upon these films. Moreover, it is striking that this rectification factor is orders of magnitude better than those typically observed in molecular donor/cceptor systems. Consideration of the origin of this remarkably asymmetric

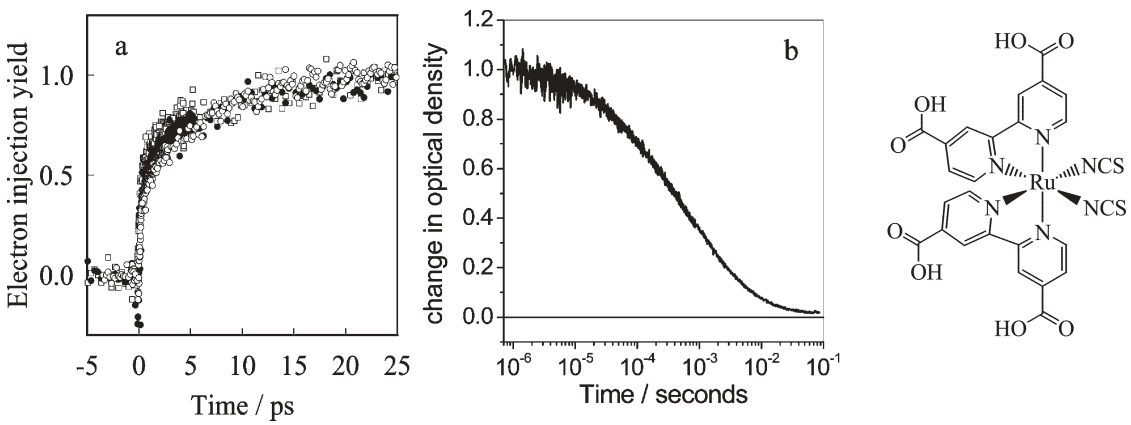

Fig. 4 Transient absorption data monitoring the dynamics of (a) charge separation and (b) charge recombination for $Ru(dcbpy)_2(NCS)_2$-sensitised TiO_2 films. Adapted from ref. 11*f*.

behaviour is therefore a obvious starting place for our discussion of electron-transfer dynamics.

Electron-transfer dynamics in molecular donor/acceptors are generally considered in terms of Marcus non-adiabatic electron-transfer theory.[12] In this theory, based upon Fermi's Golden Rule, the rate of electron injection depends upon two factors: the electronic coupling between the donor and acceptor states V^2, and the relative energetics of these states (the 'Franck–Condon factor', FC), as detailed in eqn (1). The electronic coupling depends upon the spatial overlap of donor and acceptor orbitals, and therefore follows an exponential dependence upon spatial separation r of the donor and acceptor. The exponent factor β in this term depends upon the electronic structure of the medium between the donor and acceptor species (being $\sim$1 Å^{-1} for saturated molecular systems). The Franck–Condon term corresponds to thermal activation over an activation barrier (the 'crossing point') and depends upon both free energy change resulting from the electron-transfer reaction (ΔG^0) and extent to which molecules and their environment reorganise as a result of the electron transfer (the reaction reorganization energy, λ). Energetically the reaction is most favoured (fastest) when $-\Delta G^0 \rightarrow \lambda$, (in this limit the second exponential term in eqn (1) tends to unity), corresponding to the activation barrier for the reaction tending to zero.

$$k_{ET} \propto V^2 FC \propto \exp(-\beta r)\ \exp\left(-\frac{(\Delta G^0+\lambda)^2}{4\lambda k_B T}\right)_{215} \qquad (1)$$

The only extension required to eqn (1) for dye-sensitised TiO_2 interfaces is an appreciation that the metal oxide conduction band affords a continuous band of electron-acceptor states, and therefore that comparison of theory with experiment requires a suitable integration over this density of states. Indeed the presence of this band of accepting states facilitates the achievement of activationless ($\Delta G^0 = \lambda$) electron injection and therefore rapid charge separation.

We consider first the charge separation reaction for our model system. Remarkably, despite the ultrafast dynamics of this reaction, it has proven to be relatively easy to understand the dynamics of this reaction in terms of the simple theory detailed above.[13] The direct ligation of the dye to the TiO_2 allows strong electronic coupling.[14] For the $RuL_2(NCS)_2$ sensitiser dye, this strong coupling is particularly favoured by the dye LUMO orbital from which electron injection proceeds being localised on the bipyridyl groups, and thereby in close proximity to the metal oxide surface. Studies of analogous sensitiser dyes[11d] with non-conjugated spacers between the bipyridyl rings and the TiO_2 surface have shown the expected exponential dependence of the electron-transfer rate with spacer length, as expected from eqn (1). Similarly, the rate of injection follows the expected dependence upon free energy (after suitable integration over the density of accepting states), as illustrated in Fig. 5.[11g] The dashed line shows the fit to the integrated form of eqn (1), yielding a value for $\lambda \sim 0.25$ eV, typical of values for λ for ultrafast electron-transfer reactions in both synthetic supermolecular systems and photosynthetic reaction centres.[15,16]

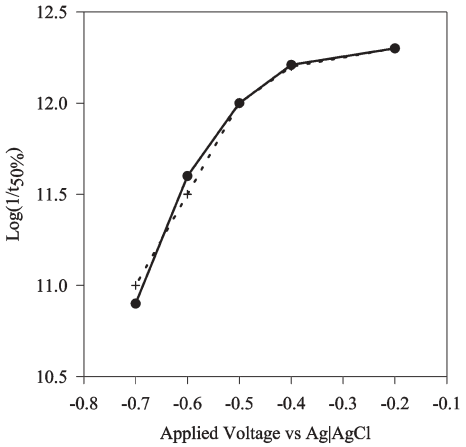

Fig. 5 Plot of experimental half-times (●) for electron injection in $RuL_2(NCS)_2$ sensitised nanocrystalline TiO_2 films as a function of the film Fermi level. The theoretical fit to this behaviour (+) was obtained by integration of eqn (1) over the density of unoccupied TiO_2 acceptor states, with a value of $\lambda \sim 0.25$ eV. (from ref. 11*g*). The non-exponential nature of the dynamics prevents us defining a formal rate constant for the injection; rather the reciprocal of the experimentally determined injection half time is used for the *y*-axis ordinate, this is proportional to the effective injection rate constant.

Understanding the remarkably slow recombination dynamics shown in Fig. 4 has proven to be a little more complex. In photosynthetic and supermolecular systems, two strategies are typically employed to retard charge recombination back to the ground state: firstly the use of a relay of redox molecules to achieve a large physical separation of the electron and 'hole' and, secondly, the selection of appropriate system energetics such that the charge recombination reaction lies strongly in the Marcus inverted region: $\Delta G^0 > \lambda$ (in this limit, the exponent of the second exponential term in eqn (1) is large and negative, resulting a slow electron-transfer rate constant). Considering the energetic approach first, studies of charge recombination in dye-sensitised nanocrystalline electrodes have indeed shown a free energy dependence in agreement with eqn (1).[17] including the observation of Marcus-inverted region behaviour, with $\lambda \sim 1$ eV, again typical of reorganisational energy observed for analogous charge-recombination dynamics in supermolecular and photosynthetic systems.[18] However for $RuL_2(NCS)_2$ sensitised TiO_2 films, the free energy difference for the charge-recombination reaction is also $\sim$1 eV, indicating that for this sensitiser dye, this reaction is not significantly into the inverted region. This observation has been supported by studies of a range of analogous sensitiser dyes where the charge recombination dynamics were observed to be only weakly dependent upon the dye ground state oxidation potential[19] (and therefore recombination reaction free energy), consistent with $|\Delta G^0| \sim \lambda$.[20]

We turn therefore to consideration of the distance dependence of electron transfer to explain the slow charge recombination dynamics shown in Fig. 1. In this respect the $RuL_2(NCS)_2$ sensitiser dye is remarkable. The long wavelength absorption band of this dye is a metal-to-ligand charge transfer (MLCT) transition from a HOMO orbital localised on the

NCS groups to a LUMO orbital localised on the bypyridyl rings. Molecular modelling studies have indicated that the dye binds to the TiO_2 surface with the NCS groups pointing away from the TiO_2 surface. This in principle results in the HOMO orbital exhibiting a large spatial separation from the TiO_2 surface, reducing the electronic coupling for the charge recombation reaction. We have recently obtained experimental confirmation of the importance of this cation localisation, employing a series of molecular analogues to the $RuL_2(NCS)_2$ dye, with dye cation HOMO orbitals varying in their spatial separation from the metal oxide surface, as illustrated in Fig. 6.[19] We found an excellent correlation between the kinetics of charge recombination, as determined by transient absorption data analogous to that shown in Fig. 4, and the spatial separation r of the dye cation HOMO orbital from the TiO_2 surface determined from semi-empirical calculations. The data show the expected exponential dependence of rate upon r, with a β value of 0.95 ± 0.2 Å^{-1}, typical of that observed for through bond electron-transfer studies of molecular donor/acceptor systems. Unsurprisingly, for this dye series, the $RuL_2(NCS)_2$ dye, which exhibits the slowest recombination dynamics, also exhibits the best photovoltaic device performance of the series. The spatial separation of HOMO and LUMO orbitals for $RuL_2(NCS)_2$ (with optical excitation in this dye resulting in a vectorial charge transfer of the electron towards the electrode surface) appears to be a key factor in achieving the high rectification factor between the charge separation and recombination dynamics as shown in Fig. 2.

In addition to the spatial localisation of the dye cation HOMO orbital away from the electrode surface, there is extensive evidence that electron trapping within the TiO_2 film also plays a key role in retarding charge recombination in this system. Such electron trapping appears to be associated with bulk rather than surface states,[21a] localising trapped electrons away from the film surface, although we note data emphasising the importance of surface trap states has recently been reported.[21b] As such, charge recombination requires thermal detrapping of the electron and transport to TiO_2 states neighbouring the dye cation, resulting in a significant retardation of the recombination dynamics. Numerical models have been developed to simulate the impact of this thermally activated detrapping upon experimentally observed recombination dynamics.[22] Such simulations have indicated an exponential energetic distribution of trap depths, in agreement with more direct studies of the trap density of states, and consistent with, for example, the non-exponential ('dispersive') recombination dynamics shown in Fig. 4.

The electron trapping dependence of the recombination dynamics in dye-sensitised metal oxide films results in the recombination dynamics being strongly dependent upon the electron density in the metal oxide, and therefore the film Fermi level E_F relative to its conduction band (or mobility) edge. As the electron occupancy is increased, electrons occupy shallower trap states and the activation barrier for detrapping is reduced, resulting in a rapid acceleration of charge-recombination dynamics, as illustrated in Fig. 7. The film Fermi level corresponds to the free energy of thermalised electrons in the film. Therefore the acceleration in recombination dynamics as a function of E_F has potentially an important impact on device function, as the increasing free energy stored (and therefore the maximal device photovoltage output) correlates with rapid acceleration of charge recombination and therefore potentially a loss of device quantum efficiency (photocurrent). We note the logarithmic acceleration of charge recombination with reaction free energy is too

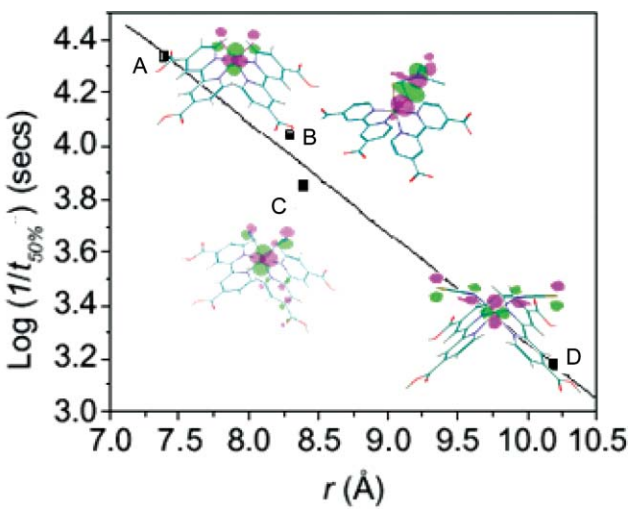

Fig. 6 Plot of the logarithm of half-times for charge recombination determined from transient absorption data *vs.* the spatial separation of dye cation HOMO orbital from the TiO_2 surface for the dye series $Ru(dcpby)_2X_2$ where X_2 = Cl_2 (A), DTC (B), $(CN)_2$ (C) and $(NCS)_2$ (D). The influence of the free energy driving force ΔG has been factored into $t_{50\%}$ data shown here to give 'free energy optimized' values. The solid line corresponds to exponential distance dependence in agreement with eqn (1). Reproduced with permission from *J. Am. Chem. Soc.*, 2004, **126**, 5225.[19] © 2004, Am. Chem. Soc.

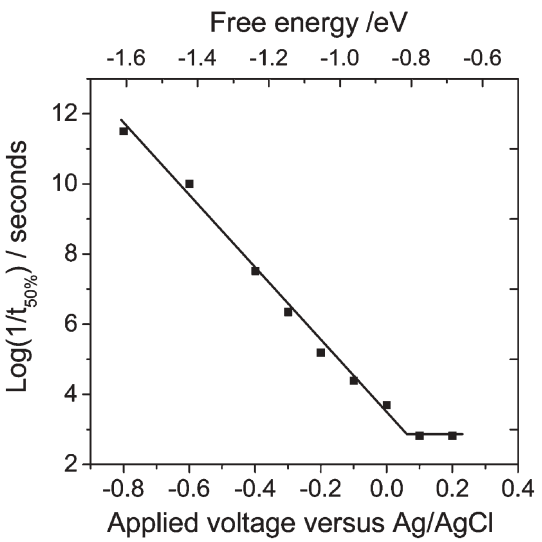

Fig. 7 Plot of the half time for charge recombination determined from transient absorption data *versus* potential applied to the TiO_2 electrode. Also shown (top axis) are the corresponding free energies of the charge separated species determined by equating the applied potential with the TiO_2 Fermi level and therefore with the electron free energy. Adapted from ref. 25*b*.

extreme to be explained by the free energy dependence of the electron-transfer rate predicted by eqn (1). We further note that this retardation of charge recombination dynamics due to electron trapping is not necessarily beneficial to device function, as the electron traps also retard the transport of electrons to the device contacts, a topic we address in detail elsewhere.[23] The influence of charge trapping upon recombination and transport dynamics also appear to be important in other molecular-based photovoltaic devices such as polymer/fullerene blends.[24] For more in depth reviews of these trapping/detrapping dynamics, and the associated transport dynamics, interested readers are referred to several recent reviews of this issue by us and others.[25]

The pre-eminence of distance rather than free energy as the parameter which can most practically be employed to achieve a long lived charge separation mirrors the situation in photosynthetic reaction centres, where studies have also emphasised the importance of distance in determining the lifetime of charge separated species.[15] This pre-eminence derives from the remarkable sensitivity of electron-transfer dynamics to spatial separation, with an increase in separation of only 0.1 nm resulting in a three-fold retardation of the electron-transfer rate constant.

From the above discussions, it is apparent that, at least for this model system, we now have some understanding of the main parameters determining the dynamics of charge separation and recombination. We now move on to consider the integration of this model system into a complete photovoltaic device.

3 Towards optimisation of electron-transfer dynamics in complete solar cells

In this section we consider electron-transfer dynamics in complete solar cells, and in particular the achievement of 'optimum' dynamics. Efficient device operation requires the photogeneration of a high yield of long-lived interfacial charge separated states. Analogous photo-induced charge separation dynamics have been extensively studied in homogeneous supermolecular structures, such as donor/acceptor systems suspended in solution.[1–3,26] Such studies have shown that the dynamics of charge separation and recombination are closely correlated, with for example modulation of the electronic coupling between the donor and acceptor by for example increasing the spacer length having equal effects upon both the charge separation and recombination dynamics. Moreover variation of the energetics of charge separation results in modulation of not only the charge separation dynamics, but also modulation of recombination dynamics both to the dyad ground and excited states. Optimisation of molecular donor/acceptor performance therefore requires careful consideration of all reaction dynamics, with for example 'optimised' electronic coupling being a compromise between being sufficiently large such that charge separation competes effectively with excited state decay, whilst being sufficiently small to minimise charge recombination.

It is becoming increasingly apparent that these issues of optimization established for supermolecular systems are of direct relevance to the optimization of molecular-based solar cells. As we have discussed above, it is possible to achieve ultrafast (sub-picosecond) charge separation in dye-sensitized nanocrystalline metal oxide films. Indeed the high photovoltaic device efficiencies achieved with such films has often been associated with the achievement of such ultrafast electron injection dynamics. In this context, it is striking that when we extended our studies of electron injection from the dye-sensitized TiO_2 film 'model system' to a complete DSSC employing an redox electrolyte empirically optimized for efficient device performance, we found that the charge separation dynamics in the optimized device were orders of magnitude *slower* than those observed for the model system, with a half time of 150 ps, as illustrated in Fig. 8.[27]

The reason for the remarkably slow injection dynamics observed for the 'optimized' DSSC device can be readily understood in terms of analogy with supermolecular systems. The lifetime of the dye excited state in the absence of electron injection is $\sim$10 ns.[11a] Efficient system function only requires that the charge separation dynamics competes effectively with this loss pathway, resulting in a near unity quantum efficiency for charge separation. As such, a 150 ps half time for electron injection is quite sufficient to achieve this. Sub-picosecond electron injection dynamics, as observed in the model system, are unnecessarily fast, they can be said to be 'kinetically redundant'. In terms of choice of electrolyte composition for optimum device performance, the minimization of charge recombination losses to both dye cations and the redox electrolyte can be more critical to device function. This is illustrated in the data in Table 1, where we determined device current/voltage characteristics and electron injection and recombination kinetics in three devices with differing electrolyte compositions. It is clear that, for this device series, the kinetics of electron injection and recombination are correlated, as observed for supermolecular systems. Optimum device performance is observed when the recombination dynamics are

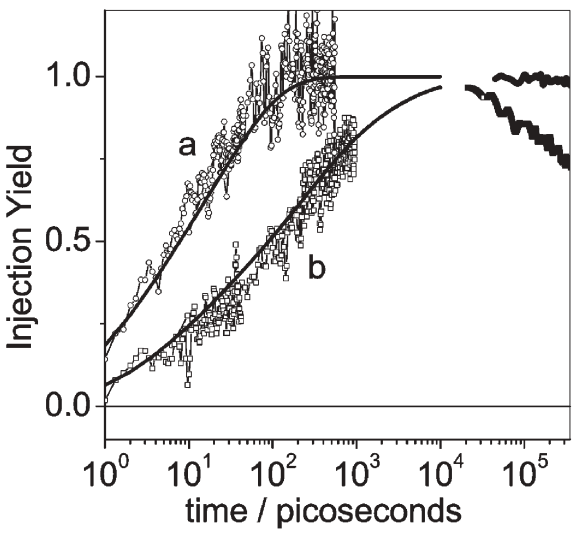

Fig. 8 Plot of the dynamics of electron injection for TiO_2 films sensitised by the di-tetrabutyl ammonium salt of $Ru(dcbpy)_2(NCS)_2$ covered (a) in an inert liquid and (b) in a typical redox electrolyte. Solid lines are the results of numerical simulations based upon a Gaussian energetic disorder model. Adapted from ref. 27.

Table 1 Table of the correlation between DSSC photovoltaic performance with charge injection and recombination dynamics. Adapted from ref. 27

	J_{sc}/mA cm^{-2}	V_{oc}/Volts	η^a (%)	$\tau_{50\%}$(inj)^b	τ_{init}(rec)^c
+Li^{+} ^{d}	16.8	0.51	5.5	~10 ps	20 ms
+Li^{+}/tBP	16.3	0.63	7.25	~150 ps	100 ms
+tBP^e	7	0.73	3.75	~1 ns	400 ms

^{a} Device efficiencies under simulated AM1.5 irradiation. ^{b} Injection half-times determined from transient absorption and emission data. ^{c} Recombination half-time determined optically following pulsed voltage excitation of the device. ^{d} Standard DSSC with 0.1 M lithium cations in the electrolyte. ^{e} Standard DSSC with 0.5 M 4-*tert*-butylpyridine.

as slow as possible whilst still allowing electron injection to be sufficiently fast to compete effectively with excited state decay. Such optimum conditions can be regarded as minimizing kinetic redundancy in the system.

It is of course not always true that charge separation and recombination dynamics in functioning devices are directly correlated. For the case shown in Table 1, the correlation arises because the changes in electrolyte composition result in shifts in the TiO_2 surface charge (*i.e.*: surface dipoles) and therefore conduction band energetics, shifting both the density of states available for electron injection and, for a given device voltage, the density of electrons in the film available for charge recombination.[14,27] Improvements in the photochemical performance of supermolecular systems has been achieved both through careful optimization of electronic coupling and energetics between specific donor/acceptor pairs, and also through increases in system complexity by, for example, the addition of the addition of secondary electron donor or acceptor species.[1] This latter approach increases the spatial separation of the electron and hole, slowing charge recombination to ground without necessarily retarding charge separation. Both approaches can, in principle, result in improvements in the efficiency of molecular-based solar cells, with the added complexity that in photovoltaic devices it is necessary to consider the dynamics of not only electron transfer but also charge transport through the device to the charge-collecting electrodes. In the final section of this article, we consider a range of molecular/materials-based approaches we are developing to achieve a systematic optimization of electron transfer and transport in such devices.

4 Interface modifications

The discussion above indicates that interfacial electron-transfer dynamics are a central to determining the efficiency of molecular-based photovoltaic devices. Optimisation of the design of this interface is therefore a key element of strategies to improve device efficiencies. In this section we will review several approaches we have been taking to improve the function of this interface. Given the nanostructured nature of this interface, all of these approaches will be based upon the self-assembly strategies to enhance the functionality of this interface. We have found that control of interfacial dynamics and subsequent improvement in device performance can be achieved by making modifications to all three components of this interface, the metal oxide, the dye structure and hole transporting material.

One of the strategies employed to improve the function of supermolecular donor/acceptor systems is the addition of secondary donor or acceptor species designed to increase the spatial separation of the final radical pair state (*e.g.*: the use of molecular 'triads' rather than dyads). We have been considering a range of strategies to emulate this functionality in DSSCs. One such approach is to use 'supermolecular' sensitiser dyes incorporating a secondary electron donor species, with the intention of increasing the physical separation of the dye cation away from the TiO_2 surface. We have had some success with this approach, using a range of different supermolecular structures, as illustrated in Fig. 9.[28] Using such approaches, we have been able to extend the lifetime of the photogenerated charge separated state up to 4 s. Moreover we have found that this lifetime is in good agreement with the simple distance *versus* lifetime relationship predicted by eqn (1), and which had seen previously for molecular sensitisers (Fig. 6, above). Studies employing such supermolecular sensitisers to improve the efficiency of dye-sensitised solar cells are currently ongoing and are already showing significant promise for solid-state devices.

We have recently extended this supermolecular approach to interface engineering to supramolecular chemistry, employing an organic sensitiser dye non-covalently encapsulated in a cyclodextrin ring (dye **5** in Fig. 9). We found cyclodextrin encapsulation of the dye results in strong binding to the nanocrystalline metal oxide electrode.[29] The encapsulation furthermore results in a well-defined spatial separation of the organic dye from the electrode surface, sufficiently close to achieve efficient electron injection, whilst being sufficiently far away to increase the lifetime of the charge separated state by an order of magnitude compared to an analogous organic dye without encapsulation.

We turn now to consideration of the metal oxide surface. One attractive approach to modulating the electronic coupling between the sensitizer dye and the metal oxide is to introduce an insulating inorganic barrier layer between these two species. Several groups, including our own, have reported procedures to conformally coat nanocrystalline TiO_2 films by a variety of insulating blocking layers including Al_2O_3, MgO and SiO_2.[30] The primary function of such blocking layers is to increase the physical separation of the injected electrons and the oxidized dye, thereby retarding the recombination reactions, although modulation of surface dipoles and passivation of surface states has also been found to be important.[31] Fig. 10 shows HRTEM images of TiO_2 particles coated with an approximately 1 nm thick layer of Al_2O_3. The alumina layer is deposited by the *in situ* hydolysis of an aluminium isopropoxide precursor on the hydrated surface of a preformed nanocrystalline TiO_2 film, resulting in the conformal growth of an Al_2O_3 barrier layer. The reader is referred elsewhere for details of the fabrication methodology.[30a] This conformal layer results in up to a 10-fold retardation in the charge recombination dynamics consistent with the blocking effect of this layer, without significantly reducing the yield of electron injection. These reduced recombination losses result in an improvement in photovoltaic device performance by up to 30%.

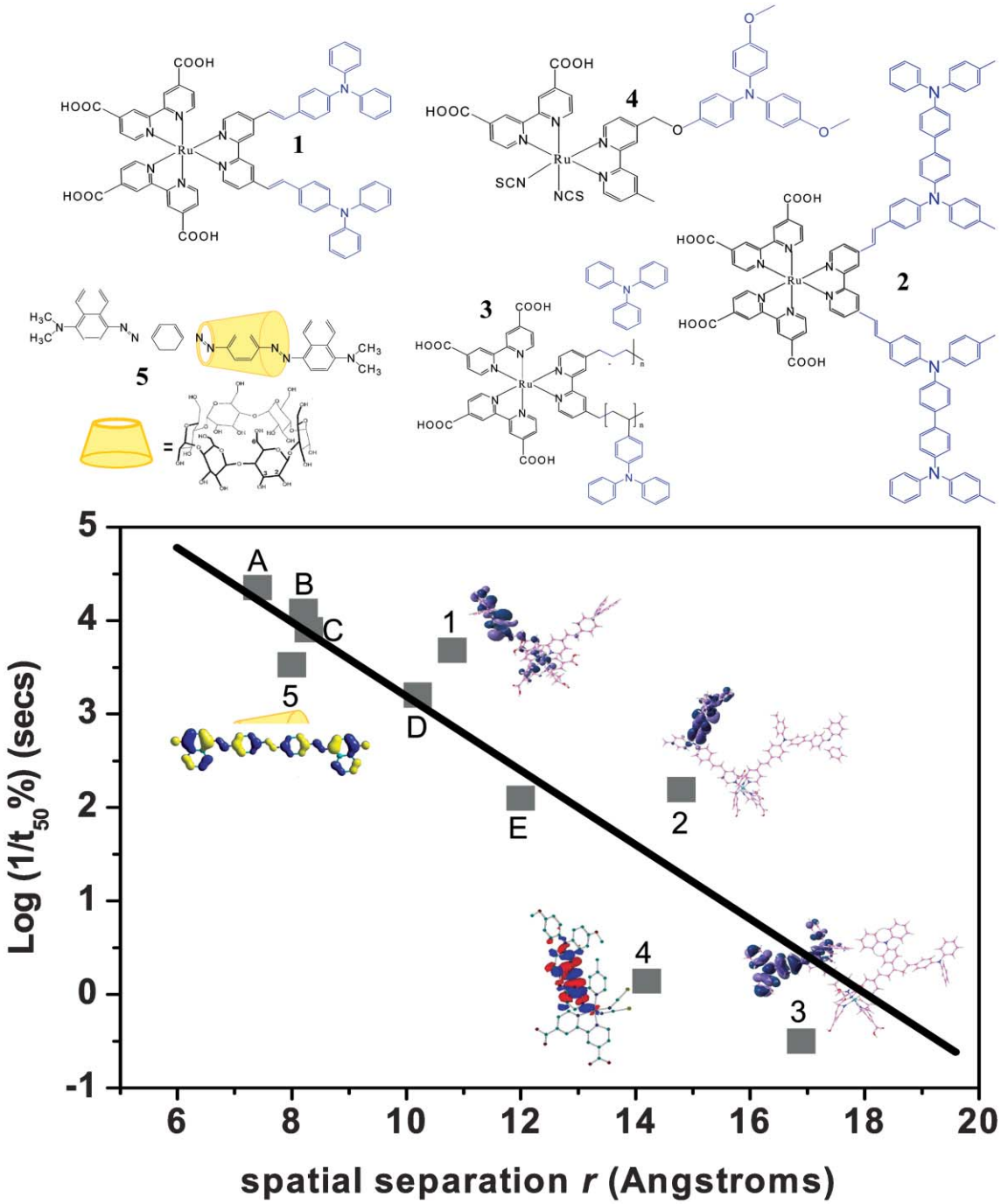

Fig. 9 Extension of the distance versus recombination half-time plot shown in Fig. 6 to supermolecular structures. Bold capital letters **A–D** correspond to the data in Fig. 6. **E** represents a Ti phthalocyanine dye from ref. 28*a*. Bold numbers **1–3** represent a series of supermolecular dyes: **1** (Ru(II)(dcbpy)$_2$(TPAbpy)), **2** (Ru(II)(dcbpy)$_2$(TPDbpy)) and **3** (Ru(II)(dcbpy)$_2$(poly-TPAbpy)) adapted from ref. 28*c*. Bold number **4** indicates a supersensitizer dye N845 adapted from ref. 28*b*, whilst **5** represents a cyclodextrin encapsulated organic dye adapted from ref. 29. The straight line is a linear fit to the experimental data following eqn (1). Adapted from ref. 28*b*.

Our initial studies of conformal growth of Al_2O_3 employed a high temperature sintering to complete the hydolysis of the aluminium isopropoxide precursor. Subsequent studies showed that this high temperature sintering was unnecessary, with simple air exposure at 100°C being sufficient to achieve a suitable blocking layer function, as illustrated in Fig. 11.[6f] This opens up the possibility of depositing the alumina layer after initial deposition of a dye monolayer. We have recently employed this strategy to achieve multilayer sensitisation of nanocrystalline TiO_2, adsorbing a second dye layer after the alumina treatment.[32] The multilater sensitisation not only resulted in enhanced sensitisation of the TiO_2 film, but also can result in the formation of a redox cascade enhancing the lifetime of the charge separated state.

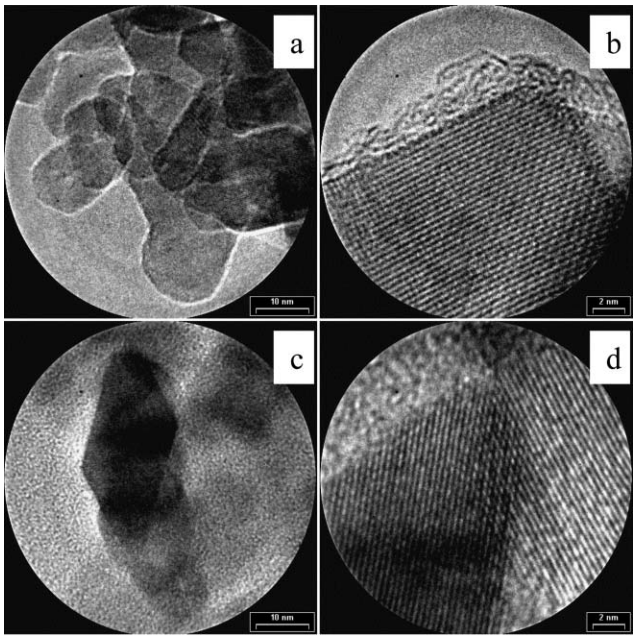

Fig. 10 HRTEMs of TiO_2 nanoparticles in presence (a, b) and absence (c, d) of an Al_2O_3 overlayer. The Al_2O_3 overlayer was grown conformally on a preformed nanocrystalline TiO_2. This film, and the uncoated control, was then broken up to a powder to allow HRTEM analysis. Pictures (b) and (d) are at high magnification. Reproduced with permission from *J. Am. Chem. Soc.*, 2003, **125**, 475.[30a] © 2003, Am. Chem. Soc.

Finally we turn to consideration of the redox electrolyte. In DSSCs, this electrolyte effectively performs a secondary electron donor function, re-reducing the photogenerated dye cation, and subsequently transporting the 'hole' (oxidised redox couple) to the counter electrode. When employing the iodide/iodine redox couple, this secondary electron-transfer functionality indeed increases the lifetime of the charge-separated state by one to two orders of magnitude.[33] This increased lifetime most probably derives not only from an increased spatial separation of the electron and 'hole' but also rather from specific two-electron chemistry required to reduce iodine to iodide at the TiO_2 surface. The reader is referred elsewhere for detailed discussions of this chemistry.[34]

The slow reduction kinetics of iodine at TiO_2 surfaces results in the iodide/iodine redox couple being particularly attractive for DSSC. Employing liquid electrolytes to achieve high ion mobilities, efficiencies of up to 11% have been reported.[5] The use of volatile liquids in a photovoltaic device is however less attractive for technological device applications. Several approaches are being considered to fabricate 'quasi-solid-state' DSSCs retaining the iodine/iodide redox couple, including the use of gelled electrolytes, ionic liquids and polymer electrolytes. Fig. 11 shows an example of one such study from our own lab, where we have employed a polyethylene oxide-based polymer electrolyte to achieve the low-temperature fabrication of DSSC on plastic substrates.[6f] The low-temperature incorporation of an alumina barrier layer results in devices efficiencies of 2.5% at one sun irradiance, increasing to 5.3% at 1/10th irradiance conditions, as illustrated in Fig. 11. In this device, the polymer employed was

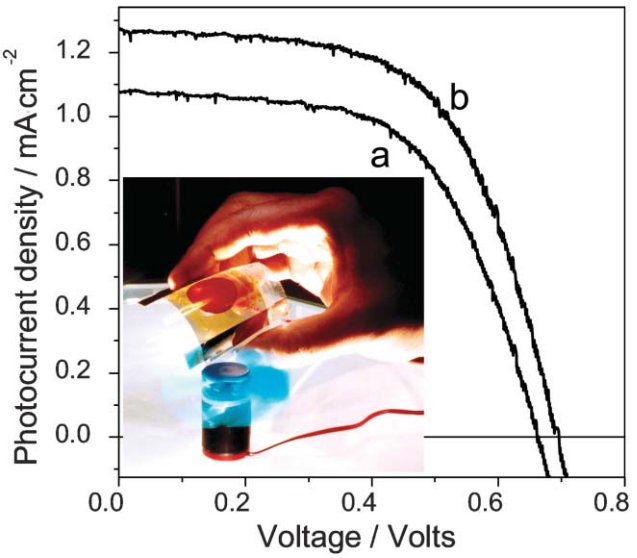

Fig. 11 Current/voltage characteristics under 10 mW cm^{-2} AM1.5 solar irradiation of flexible DSSC (see photograph) employing nanocrystalline TiO_2 films (a) and Al_2O_3 coated TiO_2 films (b) fabricated on flexible PET substrates using a polymer electrolyte, as illustrated in the inset. Adapted from ref. 6*f*.

poly-epichlorohydrin-*co*-ethylene oxide, with a molecular weight of $\sim 10^6$. Despite this high molecular weight, the polymer electrolyte readily penetrated into the film pores, attributed to favourable acid/base interactions between the polymer and the dye-sensitised TiO_2 surface.[33]

An alternative approach to the use of iodine/iodide-based electrolytes is the use of organic hole conductors. Employing the triarylamine-based semiconductor, *spiro*-OMeTAD, solid-state DSSC with efficiencies of up to $\sim$4% have been reported.[35] In such devices, charge recombination to the oxidised hole conductor is a single-electron reaction and therefore, in contrast to the iodine-based couple, exhibits similar recombination dynamics with TiO_2 electrons as the dye cation. As such, the use of interface engineering strategies to minimise recombination losses are particularly key to improving device efficiencies. We, and others, have addressed a range of strategies to achieve this, including the use of metal oxide barrier layers and the use of ambiphilic dyes with extended alkyl chains.[36] We give one example here,[37a] based upon the use of a supermolecular ion ligating, hole transporting polymer, as illustrated in Fig. 12. Insertion of the polymer with ligated Li^+ ions between the dye layer and the bulk *spiro*-OMeTAD layer (achieved by a simple dip-coating self-assembly strategy) allows the lithium ions to screen the electrostatic interactions between injected electrons and OMeTAD cations, resulting a retardation of interfacial charge recombination, and thereby an increase in device performance. This approach has recently been extended to the attachement of ion ligating groups to the molecular sensitiser dye.[38] In addition we have recently shown that this multilayer approach can be further improved by modulation of the oxidation potential of the ion ligating polymer, resulting in the formation of vectorial redox cascade at the dye/polymer/OMeTAD interface.[37b]

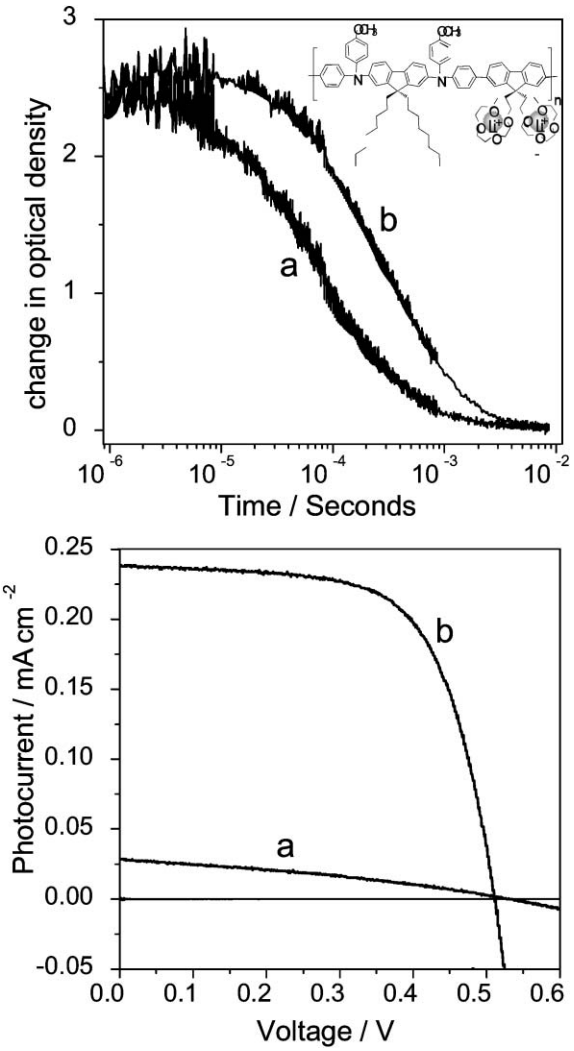

Fig. 12 Top: Transient absorption data obtained for samples $Ru(dcbpy)_2(NCS)_2$ sensitised TiO_2 /polymer/*spiro*-OMeTAD films in the absence (a) and presence (b) of $Li^+(^-NTf_2)$ in the polymer layer. The decay kinetics are assigned to the charge recombination of the OMeTAD cations with the electrons in the trap/conduction band states in the TiO_2 semiconductor. Bottom: the corresponding device current/voltage under 10 mW cm^{-2} AM1.5 solar irradiation. Adapted from ref. 33*b*

5 Conclusions

These are exciting times to be working in the field of molecular-based solar energy conversion. Academically, the field is building upon recent advances molecular and organic electronics. Commercially there is increasing interest in optoelectronic applications of organic and nanostructured electronic materials, whilst environmental concerns are motivating the quest for lower cost approaches to renewable electricity production. This article has focused on the function of one class of molecular-based photovoltaic cell, namely dye-sensitised nanocrystalline solar cells. We have shown that, building upon the parallels with natural photosynthetic reaction centres and molecular donor/acceptor systems, there is an increasingly clear scientific framework to describe at least some elements of device function. This is allowing us to move from largely empirical strategies of device optimisation to more directed 'interface engineering' strategies employing innovative molecular structures and interface processing to enhance device performance.

Technological concerns about the long-term stability of devices employing liquid electrolytes are now motivating the development of solid-state molecular photovoltaic devices, including not only solid-state dye-sensitised solar cells, but also molecular bilayer and polymer/fullerene blends. Photochemical studies of polymer/fullerene-based devices are generally less advanced, not least because the lack of control of interface morphology in such blends typically complicates the determination of clear structure/function relationships. Our initial studies have, however, already demonstrated clear parallels between the function of such blends and dye-sensitised nanocrystalline films.[24] Moreover, a range of strategies are now being developed to achieve control of interface morphology in organic donor/acceptor films,[39] allowing increasingly sophisticated approaches to the design and optimisation of such solid-state molecular photovoltaic devices.

Acknowledgements

The authors gratefully acknowledge the financial support of the EPSRC Supergen 'Excitonic Solar Cells' programme. SAH acknowledges The Royal Society for a University Research Fellowship. EP acknowledges the Spanish Ministerio de Educación y Ciencia for the Ramón y Cajal Fellowship.

Notes and references

1 (*a*) M. R. Wasielewski, *Chem. Rev.*, 1992, **92**, 435; (*b*) D. Gust, T. A. Moore and A. L. Moore, *Acc. Chem. Res.*, 2001, **34**, 40; (*c*) A. Harriman, *Angew. Chem., Int. Ed.*, 2002, **43**, 4985.

2 (*a*) K. Ohkubo, H. Kotani, J. Shao, Z. Ou, K. M. Kadish, G. Li, R. K. Pandey, M. Fujitsuka, O. Ito, H. Imahori and S. Fukuzumi, *Angew. Chem., Int. Ed.*, 2004, **43**, 853; (*b*) S. Fukuzumi, K. Ohkubo, W. E. Zhongping Ou, J. Shao, K. M. Kadish, J. A. Hutchison, K. P. Ghiggino, P. J. Sintic and M. J. Crossley, *J. Am. Chem. Soc.*, 2003, **125**, 14984; (*c*) S. D. Straight, J. Andersson, G. Kodis, A. L. Moore, T. A. Moore and D. Gust, *J. Am. Chem. Soc.*, **127**, 2717.

3 (*a*) S. Fukuzumi, K. Ohkubo, E. Wenbo, Z. Ou, J. Shao, K. M. Kadish, J. A. Hutchison, K. P. Ghiggino, P. J. Sintic and M. J. Crossley, *J. Am. Chem. Soc.*, 2003, **125**, 14984; (*b*) S. Fukuzumi, H. Kotani, K. Ohkubo, S. Ogo, N. V. Tkachenko and H. Lemmetyinen, *J. Am. Chem. Soc.*, 2004, **126**, 1600.

4 For a set of reviews, see the complete *MRS Bulletin*, 2005, vol. 30, no. 1.

5 (*a*) M. Grätzel, *Inorg. Chem.*, 2005, **44**, 6841–6851; (*b*) M. Grätzel, *Photochem. Photobiol. A*, 2004, **164**, 3.

6 (*a*) H. Wang, X. Bolei, Hong Li, Z. Wang, Q. Meug and L. Chen, *J. Am. Chem. Soc.*, 2005, **127**, 6394; (*b*) W. Ikedo and T. Miyasata, *Chem. Commun.*, 2005, 1886; P. Wang, S. M. Zakeeruddin, M. Grätzel, W. Kanthehner, J. Mezger, E. V. Stoyanov and O. Scherr, *Appl. Phys. A.*, 2004, **79**, 73; (*c*) E. Stathatos, P. Lianos, A. Surcavuk and B. Orel, *Adv. Funct. Mater.*, 2004, **14**, 45; (*d*) U. Bach, D. Lupo, P. Comte, J. E. Moser, F. Weissortel, J. Salbek, H. Spreitzer and M. Grätzel, *Nature*, 1998, **395**, 583; (*e*) B. O'Regan, F. Lenzmann, R. Muis and J. Weinke, *Chem. Mater.*, 2002, **14**, 5023; (*f*) S. A. Haque, E. Palomares, H. M. Upadhayaya, L. Otley, R. J. Potter, A. B. Holmes and J. R. Durrant, *Chem. Commun.*, 2003, 3008.

7 (*a*) C. J. Brabec and N. S. Saricifitci, *Mater. Today*, 2000, **3**, 5; (*b*) J. Nelson, *Curr. Opin. Solid State Mater. Sci.*, 2002, **6**, 87; (*c*)

C. J. Brabec, N. S. Sariciftci and J. C. Hummelen, *Adv. Funct. Mater.*, 2001, **11**, 15.
8 (*a*) F. Padinger, R. S. Rittberger and N. S. Sariciftci, *Adv. Funct. Mater.*, 2003, **13**, 85; (*b*) S. E. Shaheen, C. J. Brabec, N. Serdar Sariciftci, F. Padinger, T. Fromherz and J. C. Hummelen, *Appl. Phys. Lett.*, 2001, **78**, 841; (*c*) Y. Kim, S. Cook, S. M. Tuladhar, S. A. Choulis, J. Nelson, J. R. Durrant, D. D. C. Bradley, M. Giles, I. McCulloch, Ch.-S. Ha and M. Ree, *Nat. Mater.*, 2006, **5**, 197.
9 P. Peumans, S. Uchida and S. R. Forrest, *Nature*, 2003, **425**, 158.
10 M. K. Nazeeruddi, A. Kay, I. Rodicio, R. Humphrybaker, E. Muller, P. Liska, N. Vlachopoulos and M. Gratzel, *J. Am. Chem. Soc.*, 1993, **115**, 6382.
11 (*a*) Y. Tachibana, J. E. Moser, M. Gratzel, D. R. Klug and J. R. Durrant, *J. Phys. Chem.*, 1996, **100**, 51, 20056; (*b*) G. Benko, J. T. Kallioinen, P. Myllyperkio, F. Trif, J. R. I. Korppi-Tommola, A. P. Yartsev and V. Sundstrom, *J. Phys. Chem. B*, 2004, **108**, 2862; (*c*) J. Kallioinen, V. Lehtovuori, P. Myllyperkio and J. E. I. Korppi-Tommola, *Chem. Phys. Lett.*, 2001, **340**, 217; (*d*) N. A. Anderson, X. Ai, D. Chen, D. L. Mohler and T. Lian, *J. Phys. Chem. B*, 2003, **107**, 14231; (*e*) A. Furube, R. Katoh, K. Hara, T. Sato, S. Murata, H. Arakawa and M. Tachiya, *J. Phys Chem. B*, 2005, **109**, 16406; (*f*) Y. Tachibana, S. A. Haque, I. P. Mercer, D. R. Klug and J. R. Durrant, *J. Phys. Chem. B*, 2000, **104**, 1198; (*g*) Y. Tachibana, S. A. Haque, I. P. Mercer, J. E. Moser, D. R. Klug and J. R. Durrant, *J. Phys. Chem. B*, 2001, **105**, 7424.
12 (*a*) S. Fukuzumi, *Org. Biomol. Chem.*, 2003, **1**, 609; (*b*) R. A. Marcus and N. Sutin, *Biochim. Biophys. Acta*, 1985, **811**, 265; (*c*) C. C. Moser, J. M. Keske, K. Warncke, R. S. Farid and P. L. Dutton, *Nature*, 1992, **355**, 796.
13 N. A. Anderson and Tianquan Lian, *Annu. Rev. Phys. Chem.*, 2005, **56**, 491.
14 D. F. Watson and G. J. Meyer, *Annu. Rev. Phys. Chem.*, 2005, **56**, 119.
15 C. C. Moser, J. M. Keske, K. Warncke, R. S. Farid and P. L. Dutton, *Nature*, 1992, **355**, 796.
16 S. Fukuzumi, H. Kotani, K. Ohkubo, S. Ogo, N. V. Tkachenko and H. Lemmetyinen, *J. Am. Chem. Soc.*, 2004, **126**, 1600.
17 (*a*) D. A. Gaal and J. T. Hupp, *J. Am. Chem. Soc.*, 2000, **122**, 10956; (*b*) D. Kuciauskas, M. S. Freund, H. B. Gray, J. R. Winkler and N. S. Lewis, *J. Phys. Chem. B*, 2001, **105**, 392.
18 The larger λ observed for charge recombination compared to charge separation simply derives from the difference in timescales of these processes, with the slower timescale of charge recombination allowing much greater structural rearrangements than are possible on ultrafast timescales.
19 J. N. Clifford, E. Palomares, M. K. Nazeeruddin, M. Gratzel, J. Nelson, X. Li, N. J. Long and J. R. Durrant, *J. Am. Chem. Soc.*, 2004, **126**, 5225.
20 Utilisation of the inverted region behaviour in DSSC is typically prevented by the energy stored as charge-separated states in such devices being rarely $\gg$1 eV (with typical device output voltages in the range 0.7 V), resulting in $|\Delta G^0| \sim \lambda$. As such, the second exponential term in eqn (1) is $\sim$1, and in terms of energetics, the electron-transfer rate constant for charge recombination rate is nearly maximal. In all solid-state systems, or indeed by suitable interface design to minimise λ, it may be possible to achieve $|\Delta G^0| > \lambda$ in molecular-based photovoltaic cells, and thereby inverted region behaviour; however, studies of this issue to date have been very limited.
21 Chronoamperometric studies of trap density as a function of TiO_2 nanoparticle diameter indicate that the trap density follows the TiO_2 film volume rather than surface area: (*a*) R. Willis, PhD Thesis, University of London, 2002; (*b*) N. Kopidakis, N. R. Neale, K. Zhu, J. van de Lagemaat and A. J. Frank, *Appl. Phys. Lett.*, 2005, **87**, 202106.
22 (*a*) J. Nelson, *J. Phys. Rev.*, 1999, **59**, 15374; (*b*) J. Bisquert, *J. Phys. Chem. B*, 2002, **106**, 325; (*c*) J. Nelson and R. E. Chandler, *Coord. Chem. Rev.*, 2004, **248**, 1181.
23 A. N. M. Green, E. Palomares, S. A. Haque, J. M. Kroon and J. R. Durrant, *J. Phys. Chem. B*, 2005, **109**, 12525.
24 (*a*) J. J. Dittmer, E. A. Marseglia and H. Friend, *Adv. Mater.*, 2000, **12**, 1270; (*b*) I. Montanari, A. F. Nogueira, J. Nelson, J. R. Durrant, C. Winder, M. A. Loi, N. S. Sariciftci and Christoph Brabec, *Appl. Phys. Lett.*, 2002, **81**, 3001; (*c*) A. F. Nogueira, I. Montanari, J. Nelson, J. R. Durrant, C. Winder, N. S. Sariciftci and C. Brabec, *J. Phys. Chem. B*, 2003, **107**, 1567.
25 (*a*) S. A. Haque, Y. Tachibana, R. L. Willis, J. E. Moser, M. Grätzel, D. R. Klug and James R. Durrant, *J. Phys. Chem. B*, 2000, **104**, 538; (*b*) A. C. Fisher, L. M. Peter, E. A. Ponomarev, A. B. Walker and K. G. U. Wijayantha, *J. Phys. Chem. B*, 2000, **104**, 949; (*c*) M. Bailes, P. J. Cameron, K. Lobato and L. M. Peter, *J. Phys. Chem. B*, 2005, **109**, 15429; (*d*) A. J. Frank, N. Kopidakis and J. van de Lagemaat, *Coord. Chem. Rev.*, 2004, **248**, 1165.
26 (*a*) R. Lomoth, T. Haupl, O. Johansson and L. Hammarstrom, *Chem. Eur. J.*, 2002, **8**, 102; (*b*) H. Yamada, H. Imahori, Y. Nishimura, I. Yamazaki, T. A. Kyu, S. K. Keun, D. Kim and S. Fukuzumi, *J. Am. Chem. Soc.*, 2003, **125**, 9129; (*c*) A. C. Benniston and A. Harriman, *Chem. Soc. Rev.*, 2005, **35**, 169.
27 S. A. Haque, E. Palomares, B. M. Cho, A. N. M. Green, N. Hirata, D. R. Klug and J. R. Durrant, *J. Am. Chem. Soc.*, 2005, **127**, 3456.
28 (*a*) E. Palomares, M. V. Martínez-Díaz, S. A. Haque, T. Torres and J. R. Durrant, *Chem. Commun.*, 2004, 2112; (*b*) N. Hirata, J.-J. Lagref, E. J. Palomares, J. R. Durrant, M. K. Nazeeruddin, M. Grätzel and D. Di Censo, *Chem. Eur. J.*, 2004, **10**, 595; (*c*) S. A. Haque, S. Handa, K. Peter, E. Palomares, M. Thelakkat and J. R. Durrant, *Angew. Chem., Int. Ed.*, 2005, **44**, 2.
29 S. A. Haque, J. S. Park, M. Srinivassarao and J. R. Durrant, *Adv. Mater.*, 2004, **16**, 1177.
30 (*a*) E. Palomares, J. N. Clifford, S. A. Haque, T. Lutz and J. R. Durrant, *J. Am. Chem. Soc.*, 2003, **125**, 475; (*b*) E. Palomares, J. N. Clifford, S. A. Haque, T. Lutz and J. R. Durrant, *Chem. Commun.*, 2002, 1464; (*c*) A. Zaban, S. G. Chen, S. Chappel and B. A. Gregg, *Chem. Commun.*, 2000, 2231; (*d*) G. R. R. A. Kumara, K. Tennakone, V. P. S. Perera, A. Konno, S. Kaneko and M. Okuya, *J. Phys. D: Appl. Phys.*, 2001, **34**, 868; (*e*) K. Tennakone, J. Bandara, P. K. M. Bandaranayake, G. R. R. Kumara and A. Konno, *Jpn. J. Appl. Phys.*, 2001, **40**, L732; (*f*) A. Kay and M. Grätzel, *Chem. Mater.*, 2002, **14**, 2930.
31 F. Fabregat-Santiago, J. García-Cañadas, E. Palomares, J. N. Clifford, S. A. Haque, J. R. Durrant, G. García-Belmonte and J. Bisquert, *J. Appl. Phys.*, 2004, **96**, 6904.
32 J. N. Clifford, E. Palomares, M. K. Nazeruddin, R. Thampi, M. Grätzel and J. R. Durrant, *J. Am. Chem. Soc.*, 2004, **126**, 5670.
33 (*a*) H. M. Upadhayaya, N. Hirata, S. A. Haque, M.-A. de Paoli and J. R. Durrant, *Chem. Commun.*, 2006, 877; (*b*) A. F. Nogueira, J. R. Durrant and M. A. De Paoli, *Adv. Mater.*, 2001, **13**, 826; (*c*) I. Montanari, J. Nelson and J. R. Durrant, *J. Phys. Chem. B*, 2002, **106**, 12203.
34 (*a*) A. N. M. Green, R. E. Chandler, S. A. Haque, J. Nelson and James R. Durrant, *J. Phys. Chem. B*, 2005, **109**, 142; (*b*) A. C. Fisher, L. M. Peter, E. A. Ponomarev, A. B. Walker and K. G. U. Wijayantha, *J. Phys. Chem. B*, 2000, **104**, 949; (*c*) S. Y. Huang, G. Schlichthorl, A. J. Nozik, M. Gratzel and A. J. Frank, *J. Phys. Chem. B*, 1997, **101**, 2576.
35 (*a*) U. Bach, D. Lupo, P. Compte, J. E. Moser, F. Weissortel, J. Salbeck, H. Spreitzer and M. Gratzel, *Nature*, 1998, **395**, 583; (*b*) L. Schmidt-Mende, U. Bach, R. Humphry-Baker, T. Horiuchi, M. Miura, S. Ito, S. Uchida and M. Grätzel, *Adv. Mater.*, 2005, **125**, 813.
36 L. Schidt-Mende, J. E. Kroeze, James R. Durrant, Md. K. Nazeeruddin and M. Grätzel, *Nano Lett.*, 2005, **5**, 1315.
37 (*a*) S. A. Haque, T. Park, C. Xu, S. Koops, N. Schulte, R. J. Potter, A. B. Holmes and J. R. Durrant, *Adv. Funct. Mater.*, 2004, **14**, 435; (*b*) N. Hirata, J. Kroeze, T. Park, D. Jones, S. A. Haque, A. B. Holmes and J. R. Durrant, *Chem. Commun.*, in press.
38 Henry J. Snaith, Shaik M. Zakeeruddin, L. Schidt-Mende, Cedric Klein and M. Grätzel, *Angew. Chem., Int. Ed.*, 2005, **44**, 6413.
39 (*a*) K. Sivula, Z. T. Ball, N. Watanabe and J. M. J. Frechet, *Adv. Mater.*, 2006, **18**, 206; (*b*) S. M. Lindner and M. Thelakkat, *Macromolecules*, 2004, **37**, 8832.